Journal of Power Sources 195 (2010) 1136–1141

Contents lists available at ScienceDirect

Journal of Power Sources

journal homepage: www.elsevier.com/locate/jpowsour

Water incorporation and proton conductivity in titanium substituted barium indate

Eric Quarez*, Samuel Noirault, Maria Teresa Caldes, Olivier Joubert

Institut des Matériaux Jean Rouxel (IMN), Université de Nantes, CNRS, 2, rue de la Houssinière, BP 32229, 44322 Nantes Cedex 3, France

ARTICLE INFO

Article history:
Received 22 April 2009
Received in revised form 29 July 2009
Accepted 29 August 2009
Available online 6 September 2009

Keywords:
Oxide perovskite
Oxygen vacancies
Hydration
Anionic and proton conductivities
SOFC

ABSTRACT

Water uptake in the perovskite-like oxygen deficient compounds $Ba_2(In_{1-x}Ti_x)_2O_{5+x}\square_{1-x}$ ($0 \le x < 0.7$) (called BIT*x*) was investigated by thermal gravimetric analysis (TGA) at equilibrium conditions and thermodynamic data of the hydration process were extracted. The change of the lattice volume upon hydration, inferred from X-ray diffraction data, appears as an important parameter for the characterization of perovskite-type proton conductors. The proton conductivity, the transport number and the proton diffusion coefficients for BIT*x* compounds were determined from conductivity measurements performed under wet and dry atmosphere. The conductivity of $Ba_2(In_{1-x}Ti_x)_2O_{5+x}\square_{1-x}$ compounds is mainly protonic up to 450 °C and the best level of proton conductivity was obtained for BIT02 with a value of 1.1×10^{-3} S cm^{-1} at 450 °C.

1. Introduction

Practical application of solid oxide fuel cell (SOFC) technology at large scale requires a decreasing of the operating temperature range down to 500–800 °C. One solution relies on the use of a high temperature proton conductor oxide as electrolyte. Indeed, the lower activation energy for the protonic conduction compared to that of the oxygen ion conduction allows the lowering of the operating temperature. Moreover, when a proton conductor is used for SOFC instead of an oxide-ionic conductor, no water molecule is generated at the fuel electrode, avoiding fuel dilution and therefore increasing its efficiency. Numerous oxygen deficient oxides have been found to dissolve significant amounts of protons by equilibration with water vapor involving the filling of oxygen vacancies and the replacement of their effective positive charge by protons as hydroxide ions. Consequently, they can show useful proton conduction at intermediate or elevated temperature in wet atmospheres, with possible application as electrolyte in a proton ceramic fuel cell (PCFC). Proton-conducting oxide electrolytes for PCFC application are generally doped perovskites such as doped barium cerate compounds which have drawn the main attention up to now for their high proton conductivity – about 10^{-2} S cm^{-1} at 500 °C. The main dopants are Nd [1,2], Gd [3–7], Y [8–14] or Sm [15,16]. But this type of materials tends to exhibit high basicity with poor chemical and mechanical stability. In search of more stable proton-conducting materials for an equivalent proton conductivity level, we investigated materials based on doped barium indate oxide.

In previous studies, we have shown that the progressive filling of oxygen vacancies in the brownmillerite compound $Ba_2In_2O_5$, concomitant with substitution of Ti for In in $Ba_2(In_{1-x}Ti_x)_2O_{5+x}\square_{1-x}$ ($0 \le x \le 0.7$) (called BIT*x*), induces a disorder within the initially ordered array of such vacancies [17]. Thus, for a substitution rate larger than 15%, all compounds adopt a disordered cubic perovskite structure at room temperature exhibiting better anionic conductivity than the parent $Ba_2In_2O_5$ phase. $Ba_2In_{2(1-x)}Ti_{2x}O_{5+x}$ ($0 \le x \le 1$) compounds react with water vapor at ~300 °C to produce $Ba_2In_{2(1-x)}Ti_{2x}O_{4+2x}(OH)_y$ ($0 \le x \le 1$; $y \le 2(1-x)$) phases [18]. Under wet atmosphere, this class of materials contains sufficient equilibrium concentrations of protons to exhibit proton conduction at moderate temperatures.

In the present article, the hydration process of BIT*x* compounds and in particular BIT02 was studied by TGA and X-ray thermodiffractometry allowing the authors to extract thermodynamic data and to characterize the structural transition induced by the water uptake. The BIT*x* compounds were subjected to conductivity measurements under wet and dry atmosphere leading to the determination of the proton conductivity, the transport number and the proton diffusion coefficient. The conductivity of BIT*x* compounds is mainly protonic up to 400–500 °C depending on the Ti content and the highest proton conductivity of approximately 10^{-3} S cm^{-1} was found for BIT02 at 500 °C. We demonstrate that BIT*x* compounds can be considered as candidates for PCFC applications.

* Corresponding author. Tel.: +33 2 40 37 39 13; fax: +33 2 40 37 39 95.
E-mail address: eric.quarez@cnrs-imn.fr (E. Quarez).

0378-7753/$ – see front matter © 2009 Elsevier B.V. All rights reserved.
doi:10.1016/j.jpowsour.2009.08.086

2. Experimental

2.1. Synthesis

$Ba_2(In_{1-x}Ti_x)_2O_{5+x}\square_{1-x}$ ($0 \le x < 0.7$) compounds were prepared by solid state reaction in air from $BaCO_3$, In_2O_3 and TiO_2 as described earlier in [17]. Stoichiometric mixtures of the reactants, according to the cation stoichiometry of the BIT*x* compound, were ground in mortar and heated at 1200 °C for 24 h. The products were then compacted in pellets and heated at 1350 °C for 24 h. Part of the products was manually ground in mortar and passed through a 100 μm sieve in order to carry out TGA and XRD studies. For the conductivity measurements, a further grinding using a FRITSCH P7 planetary micro mill during 4 h at 500 rpm was necessary. Dense pellets (>95% of the theoretical density) were obtained by compacting the ground powder under a pressure of 150 MPa and sintered at 1400 °C for 48 h.

2.2. Thermogravimetric analyses of the anhydrous phases

As all compounds might have reacted with water vapor during the synthesis while being cooled down to RT, the preparation of anhydrous phases includes a dehydration step at 700 °C for 2 h under dynamic vacuum, which is maintained until cooling down to RT.

TGA measurements were carried out on ~40 mg of powder of different members of the barium indate $Ba_2(In_{1-x}Ti_x)_2O_{5+x}\square_{1-x}$ ($0 \le x < 0.7$) family using a PerkinElmer Model TGS-2 TGA system. Wet air was obtained by passing the gas through a glass tube containing distilled water at 20 °C ($p_{H_2O} = 0.023$ atm).

2.3. X-ray studies

To record data as a function of temperature, we used a Brüker "D8 Advance" powder diffractometer equipped with an Anton Paar 1200N high temperature attachment. Data were collected in Bragg-Brentano geometry with a Cu-anode X-ray source, but no monochromator was used. The detector was a 1D silicon-strip PSD (LynxEye detector) and the Cu Kbeta radiation was filtered by means of a Ni foil. An X-ray diffraction pattern of the $BaIn_{0.8}Ti_{0.2}O_{2.6}$ (BIT02) powder was first recorded at room temperature, followed by patterns recorded under wet atmosphere from 850 °C to RT every 50° between 850 and 400 °C and every 20° between 400 and 200 °C. The last X-ray diffraction patterns were recorded at 175, 150, 100 and 25 °C. Between each fixed temperature, the powder was cooled down at a rate of 0.5 °C min^{-1}. For each temperature and to be certain the system reached equilibrium conditions, 3 consecutive XRD patterns were recorded except at 280, 260, 240 and 220 °C where 5 patterns were recorded. Similar experiments were performed for BIT04 and BIT06 samples. Refinements of cell parameters were carried out using the program FULLPROF [19] in the full pattern matching mode and its interface: the program WinPLOTR [20].

2.4. Conductivity measurements

The conductivity measurements were made on samples pressed in the form of pellets, using model 1260 Frequency Response Analyzer of M/s Solartron (Schlumberger, UK) with 100 mV of ac perturbation, from 2 MHz to 0.01 Hz, between 25 and 800 °C, in dry and wet N_2 ($p_{H_2O} = 0.023$ atm). Both sides of the pellets were coated with Pt paste acting as electrodes. The complex impedance spectra were analyzed using commercially available Z-View software (Scribner Associates Inc.).

3. Results and discussion

3.1. TGA studies and thermodynamics of water uptake in BITx

In order to reach the equilibrium conditions for the hydration process, each anhydrous compound was subjected to cooling step from 800 °C to RT in a thermogravimetric (TG) apparatus under wet air at 0.1 K min^{-1} cooling rate.

When oxygen deficient oxides such as $Ba_2(In_{1-x}Ti_x)_2O_{5+x}\square_{1-x}$ dissolve protons by contact with water vapor, the reaction involves the filling of oxygen vacancies and the replacement of their effective positive charge by protons as hydroxide ions [21,22]. This reaction can be written as:

$$Ba_2In_{2(1-x)}Ti_{2x}O_{5+x}\square_{1-x} + nH_2O \rightarrow Ba_2In_{2(1-x)}Ti_{2x}O_{5+x-n}\square_{1-x-n}(OH)_{2n} \quad (1)$$

According to reaction (1), the weigh gain obtained from TG measurements at each temperature can be expressed in terms of *n*(OH) content (see Fig. 1a). The incorporation of water occurs in two steps: a very slow process is observed at high temperature whereas the reaction becomes much faster below leading to fully

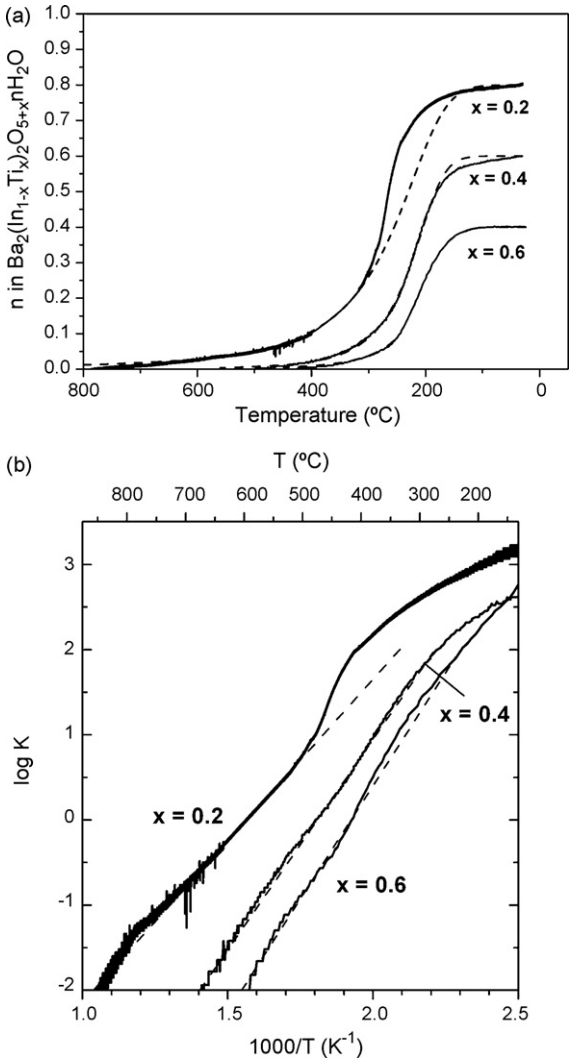

Fig. 1. (a) Hydration behavior of $Ba_2(In_{1-x}Ti_x)_2O_{5+x}\square_{1-x}$ ($x = 0.2$, 0.4 and 0.6) compounds recorded at 0.1 K min^{-1} under wet air. Simulated hydration curves are represented in dotted line. The thermodynamic parameters have been obtained by assuming Van't Hoff behavior (Eq. (5)). (b) Equilibrium constant of the hydration reaction as calculated by Eq. (4) for $Ba_2(In_{1-x}Ti_x)_2O_{5+x}\square_{1-x}$ ($x = 0.2$, 0.4 and 0.6).

hydrated phases at low temperature. The temperature range of the fast hydration step decreases when x increases. In these compounds, the basicity is mainly driven by the presence of barium. For the same barium content, the basicity depends on the difference of electronegativity between Ti^{4+} and In^{3+}. The electronegativity of Ti^{4+} being higher than the one of In^{3+}, the total basicity will decrease with titanium content. Thus, since Ti-poor samples such as BIT02 are more basic than Ti-rich ones, they will react with water vapor upon cooling at higher temperature.

In the Kröger–Vink notation, reaction (1) can be denoted by the following equilibrium reaction:

$$H_2O(g) + O_O^x + V^{\bullet\bullet} \leftrightarrow 2OH^{\bullet} \quad (2)$$

for which the equilibrium constant is:

$$K = \frac{[OH^{\bullet}]^2}{p_{H_2O}[V^{\bullet\bullet}][O_O^x]} \quad (3)$$

assuming that the hydration process can be considered as a single-phase reaction (solid solution). According to Eq. (1), K can be written as:

$$K = \frac{(2n)^2}{0.023(1-x-n)(5+x-n)} \quad (4)$$

and this latter equation can be used to calculate K from each data point of hydration curves such as those presented in Fig. 1a assuming that the maximum water uptake corresponds to the number of oxygen vacancies (i.e. $1-x$). Calculated values presented in Fig. 1b show a Van't Hoff behavior in a large temperature range for the three compositions. For $x = 0.2$, the hydration process shows a deviation from linearity at low temperature (~400 °C) indicating that the hydration is not a single-phase process [23].

The linear parts of the hydration curves were used to determine the standard hydration enthalpies (ΔH_{hydr}) and entropies (ΔS_{hydr}) for each composition according to:

$$RT \ln K = T\,\Delta S_{hydr} - \Delta H_{hydr} \quad (5)$$

The correlation between ΔS_{hydr} and ΔH_{hydr} for $x = 0.2$, 0.3, 0.4 and 0.6 compounds is plotted in Fig. 2. The dehydration isotherms (straight lines) indicate the thermodynamical stability of protonic defects $OH^{\bullet}$ ($\Delta G^{\circ} = 0$). The ΔS_{hydr} increases with ΔH_{hydr}, however, hydration enthalpy evolution, from low to Ti-rich samples, is not in agreement with the decreasing basicity. Actually, the hydration enthalpy is not only related to the basicity of the compounds but another contribution corresponding to the enthalpy of oxygen vacancies formation (ΔH_V) needs to be added to the enthalpy of hydroxyl groups formation (ΔH_{OH}) according to:

$$\Delta H_{hydr} = \Delta H_{OH} - \Delta H_V \quad (6)$$

Therefore, ΔH_V plays a predominant role during the hydration process eclipsing the influence of basicity behavior of the compounds.

ΔS_{hydr} and ΔH_{hydr} were used to simulate the hydration curves, and as can be seen in Fig. 1a simulated hydration curves fit quite well with the experimental ones in a large temperature range for $x = 0.4$ and 0.6. This means that, for $x > 0.2$ compounds, the hydration process occurs as a single-phase process. However, for BIT02, the experimental curve cannot be fitted with the standard hydration enthalpies and entropies from 150 to 300 °C. This feature is probably due to a multi-phase hydration process.

In order to characterize the structural transition induced in these compounds by the water uptake process a thermodiffactometry study was performed.

3.2. Thermodiffractometry studies

A further proof that the hydration process induces structural modifications for BIT02 compound was given by X-ray thermodiffractometry. The powder sample was heated at 800 °C in wet air (2.5% H_2O) and cooled down to room temperature by steps. XRD patterns were recorded at each step after 3–5 h in order to reach equilibrium. As can be seen in Fig. 3, from 850 to 250 °C, the XRD patterns can be indexed in a cubic cell ($Pm\bar{3}m$ space group). However, at 240 °C, one set of peaks corresponding to a tetragonal symmetry appears and is added to the set of peaks of the cubic phase. From 220 °C to RT, the totality of the peaks in each XRD pattern was indexed in the tetragonal symmetry. The powder obtained at RT was subsequently subjected to a TGA analysis showing that the thermodiffraction experiment led to a fully hydrated phase $BaIn_{0.8}Ti_{0.2}O_{2.2}(OH)_{0.8}$.

The evolutions of the cell volume as a function of temperature is represented in Fig. 4a and interpreted according to the TG analysis reported above. This correlation can be done because both XRD and TG studies were made at thermal equilibrium. At high temperatures, the linear part corresponds to the thermal evolution of the cubic dry phase $BaIn_{0.8}Ti_{0.2}O_{2.6}\square_{0.4}$

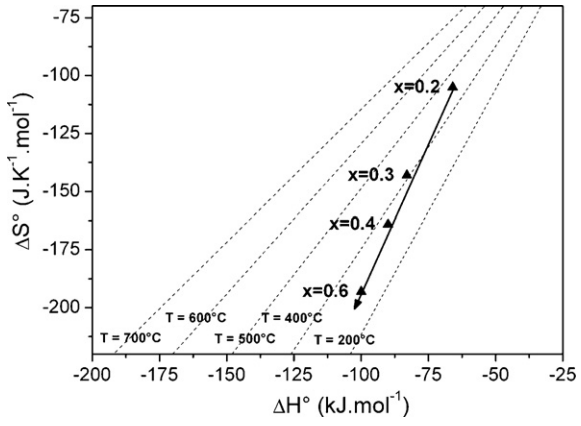

Fig. 2. Thermodynamics data of the hydration reaction for $Ba_2(In_{1-x}Ti_x)_2O_{5+x}\square_{1-x}$ ($x = 0.2, 0.3, 0.4$ and 0.6) compounds. The arrow indicates the direction of the decreasing number of vacancies. The straight lines correspond to the plots of the equations $\Delta S^{\circ} = \Delta H^{\circ}/T$ (i.e. $\Delta G^{\circ} = 0$) at different temperatures.

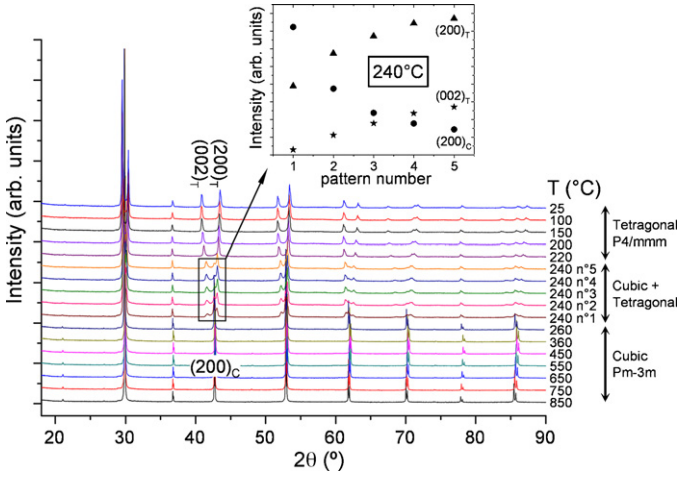

Fig. 3. X-ray diffraction patterns as a function of temperature for $BaIn_{0.8}Ti_{0.2}O_{2.6}\square_{0.4}$ during the hydration process. The inset represents the evolution at 240 °C of the cubic and tetragonal phases proportion through the intensity of characteristic peaks showing the progressive disappearing of the cubic phase accompanied with the progressive appearance of the tetragonal phase.

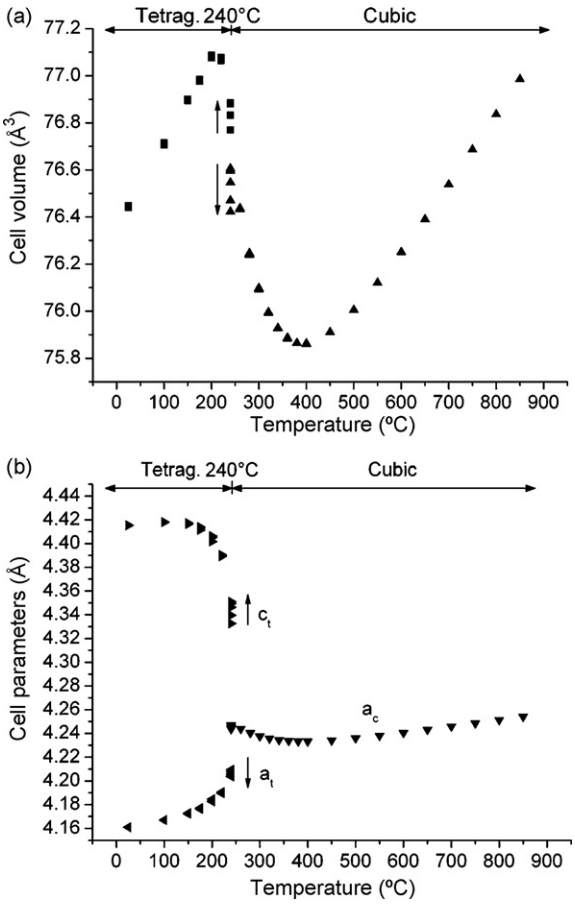

Fig. 4. Evolution of the cell volume (a) and cell parameters (b) as a function of temperature for $BaIn_{0.8}Ti_{0.2}O_{2.6}\square_{0.4}$ during the hydration process. The arrows indicate the evolution of the cell volume and parameters obtained for the consecutive patterns done at 240 °C.

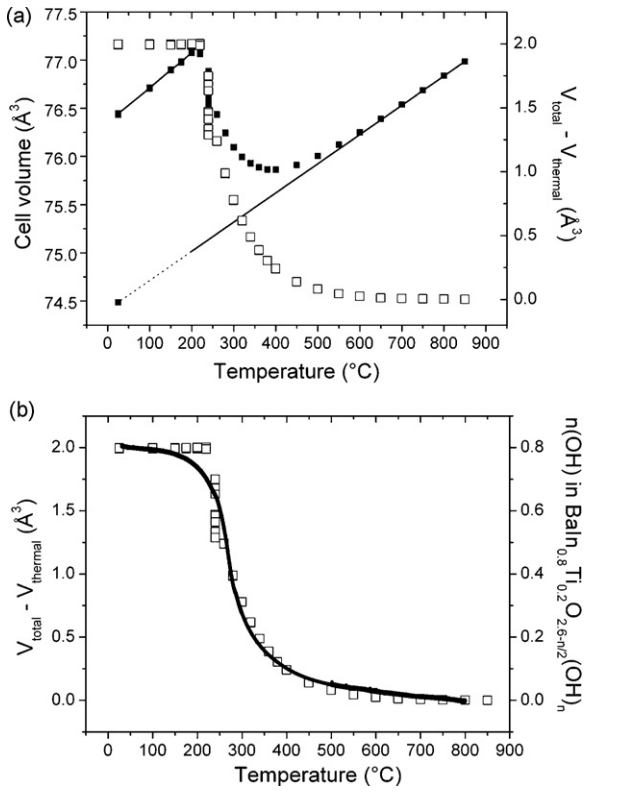

Fig. 5. (a) Chemical expansion ($\Delta V = V_{total} - V_{thermal}$) due to hydration in $BaIn_{0.8}Ti_{0.2}O_{2.6}\square_{0.4}$. Linear contributions at high and low temperature correspond, respectively, to the thermal contraction of the cubic dry phase $BaIn_{0.8}Ti_{0.2}O_{2.6}\square_{0.4}$ and of the tetragonal fully hydrated phase $BaIn_{0.8}Ti_{0.2}O_{2.2}(OH)_{0.8}$. These thermal contractions were subtracted from the total volume (black points) leading to the open squares. The volume at RT of the powder before running the thermal experiment is also reported ($V_{cubic} = 74.64$ Å^3) and is included on the extrapolation of the cubic thermal contraction. (b) Chemical expansion and number of proton incorporated n(OH), during the hydration process, as a function of temperature. A good agreement is observed.

whose thermal expansion coefficient (TEC) can be calculated and is about 12.5×10^{-6} K^{-1}. From 500 °C, a deviation from linearity due to the hydration process is observed. The symmetry of the hydrated $BaIn_{0.8}Ti_{0.2}O_{2.6-n/2}\square_{0.4-n/2}(OH)_n$ ($0 < n < 0.65$) solid solution remains cubic down to 240 °C where a mixture of cubic and tetragonal phases is present. From below 240–200 °C, the hydration and thermal evolution of the hydrated $BaIn_{0.8}Ti_{0.2}O_{2.6-n/2}\square_{0.4-n/2}(OH)_n$ ($0.65 < n < 0.8$) solid solution with tetragonal symmetry take place. Below 200 °C, the linear part corresponds to the thermal evolution of the fully hydrated phase $BaIn_{0.8}Ti_{0.2}O_{2.2}(OH)_{0.8}$ (TEC = 14.1×10^{-6} K^{-1}). The modification of the symmetry from cubic to tetragonal is not, strictly speaking, a phase transition as the composition varies with the protons incorporated within the structure. One should speak in this case of phase transformation.

At $T = 240$ °C, the level of hydration of the cubic phase reaches a maximum involving a transformation from cubic to tetragonal symmetry. For each XRD pattern done consecutively at the same temperature, the cubic phase progressively vanishes (inset Fig. 3), associated with a volume decreasing (Fig. 4), to the profit of the tetragonal one whose volume gradually increases, the variation of volume being due to hydration/dehydration process. The phase transformation is here not directly activated by the temperature but by the hydration level of the cubic phase meaning that, if the equilibrium conditions are not reached, the cubic phase may co-exist with the tetragonal one below 240 °C.

Fig. 4b exhibits the evolution of the cell parameters of BIT02 as a function of the temperature. The cubic a_c cell parameter shows the same evolution as the cubic volume upon cooling. From 240 °C to RT, the tetragonal a_t cell parameter is continuously decreasing whereas the c_t cell parameter is continually increasing meaning that the dissolution of protons within the network may induce structural reorganization such as octahedral tilting and rotations leading to an extension along the c axis and a contraction of the tetragonal basis. One can note that the temperature of phase transformation clearly corresponds to the temperature range where the fit of the TG trace is not good in Fig. 1a.

In Fig. 5a, linear contributions of the thermal evolution of the anhydrous phase at high temperature and of the fully hydrated phase at low temperature were subtracted from the cell volume (black points). The resulting curve materialized by open squares ($\Delta V = V_{total} - V_{thermal}$) corresponds to the chemical expansion exclusively due to the hydration process in BIT02 sample. This curve can be plotted as a function of the temperature on the same graph as the one representing the proton content (nOH) in BIT02 deduced from the TGA study (Fig. 5b). One can note that the ΔV and n(OH) curves fit perfectly with each other meaning that chemical expansion is clearly related to the proton incorporation process.

Concerning BITx compounds with $x > 0.2$, X-ray thermodiffractometry studies did not show any phase transformation upon cooling from 800 °C to RT. The symmetry remains cubic ($Pm\bar{3}m$ space group) throughout the experiments.

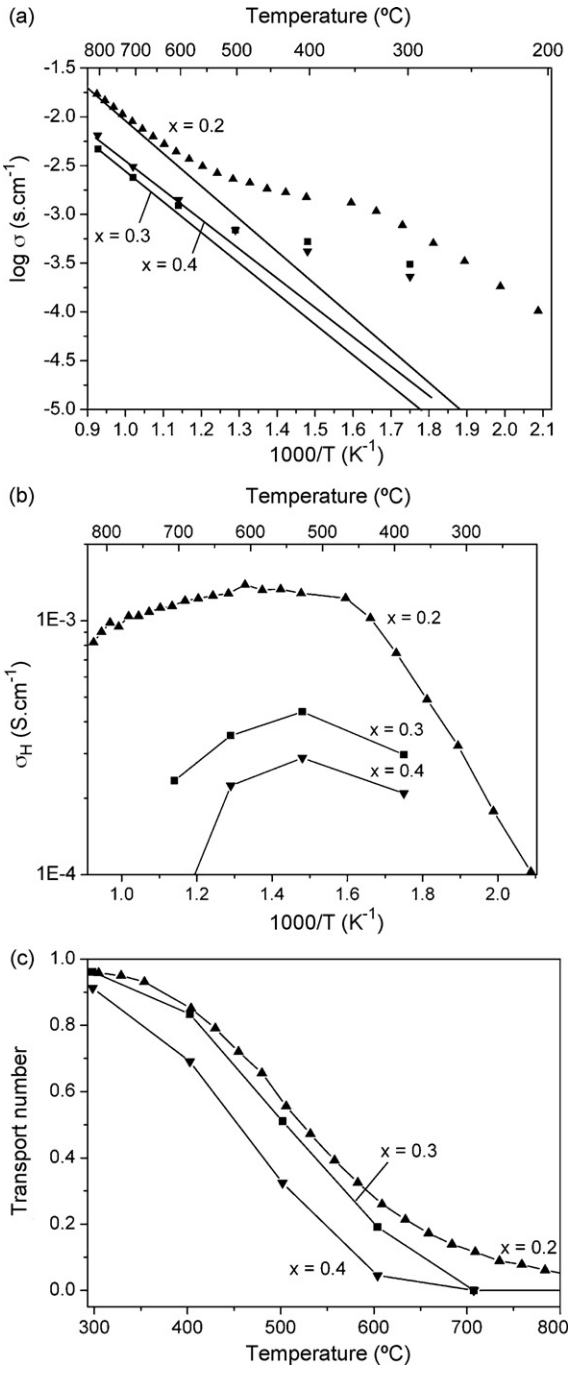

Fig. 6. Total conductivity as a function of inverse absolute temperature under dry (lines) and wet N_2 (symbols) (a), proton conductivity σ_H ($\sigma_H = \sigma_{wet} - \sigma_{dry}$) as a function of inverse absolute temperature (b) and evolution of the transport number as a function of temperature (c) for $Ba_2(In_{1-x}Ti_x)_2O_{5+x}\square_{1-x}$ ($x = 0.2$, 0.3 and 0.4) compounds.

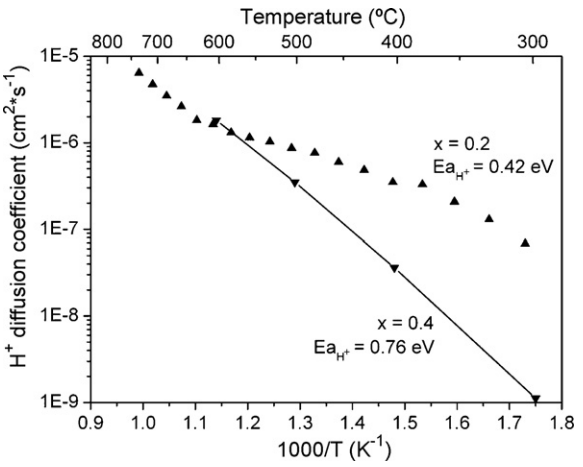

Fig. 7. Proton diffusion coefficient as a function of inverse absolute temperature for $Ba_2(In_{1-x}Ti_x)_2O_{5+x}\square_{1-x}$ ($x = 0.2$ and 0.4) compounds. The activation energy for $x = 0.2$ was calculated between 300 and 375 °C.

3.3. Conductivity measurements

Conductivity measurements were performed for several compositions ($x = 0.2$, 0.3 and 0.4). The results are presented in the form of Arrhenius plots in Fig. 6a. Under dry N_2, the good level of anionic conductivity at high temperature is confirmed [17] and is significantly superior to the one of $Ba_2In_2O_5$ which is about 2×10^{-4} S cm^{-1} at 700 °C. Upon cooling, in wet N_2 atmosphere ($p_{H_2O} = 0.023$ atm), the data show an increase in the conductivities in comparison with measurements in dry atmosphere. This is in agreement with the hydration behavior. At low temperature, the proton contribution is clearly seen for the three compositions. If we do the approximation that the O^{2-} conductivity level is the same in the anhydrous and hydrated phases at the same temperature then proton conductivity (σ_{H+}) can be obtained by subtracting the conductivity of the material in dry atmosphere (σ_{dry}) to the conductivity in wet atmosphere according to $\sigma_{H+} = \sigma_{Total} - \sigma_{O^{2-}} = \sigma_{wet} - \sigma_{dry}$ [24]. Fig. 6b shows the evolutions of the calculated proton conductivity. The maximum proton conductivity is about 1.1×10^{-3} S cm^{-1} between 450 and 600 °C for $BaIn_{0.8}Ti_{0.2}O_{2.6-n/2}\square_{0.4-n/2}(OH)_n$. For a given temperature, the proton conductivity decreases when substitution ratio increases. In the studied temperature range, an increase of the proton conductivity with the increasing temperature is observed until to reach a maximum followed by a decrease of the proton conductivity at high temperature. These non-linear variations are due to the competition between the decrease of the number of protons and the increase of their mobility when temperature increases. The evolution of the transport number of the protons permits to better exemplify the evolution of the protonic contribution to the total conductivity (Fig. 6c). For all compositions, there is a regular decrease of the transport number with the temperature related to the decrease of the number of charge carriers in the compounds. The evolution of the transport number follows the same trend than the hydration process observed in Fig. 1a: at a given temperature, the transport number decreases with the substitution ratio.

3.4. Evaluation of proton diffusion coefficient

The thermal gravimetric analyses permit to follow the hydration process and to determine the number of charge carriers involved in the proton conduction ($OH^{\bullet}$). The conductivity measurements performed under wet and dry atmosphere permit to separate the different contributions namely anionic and protonic. The diffusion of the different charge carriers within the material can be determined using the Nernst-Einstein relation and the results of the thermogravimetry and proton conductivity studies [25]. The diffusion coefficient follows an Arrhenius law for $x = 0.4$ in the full temperature range but for $x = 0.2$, it clearly appears slope changes which are probably related to the phase transformation observed at 240 °C by X-ray thermal diffraction (Fig. 7). The activation energies of proton diffusion, calculated for $x = 0.2$ between 300 and 375 °C, are also included in the graph. The obtained values are similar to those of the literature [26] and relatively low confirming the good

ability for protons to migrate in these materials. The increase of the activation energies with substitution ratio is in agreement with the increase of the covalence of the bond (In, Ti)–O.

4. Conclusion

The hydration process in $Ba_2(In_{1-x}Ti_x)_2O_{5+x}\square_{1-x}$ ($x = 0.2$, 0.4 and 0.6) compounds were studied by TG analysis. A thermodynamic approach of this hydration process shows that it is not a single-phase reaction for $x = 0.2$. Thermal XRD analysis carried out on BIT02 compound, under wet atmosphere, shows upon cooling, a phase transformation from cubic to tetragonal symmetry at 240 °C. A correlation between the chemical expansion in BIT02 due to the hydration process, inferred from XRD data, and the number of protons incorporated within the network, obtained by TGA analysis, has been established. The conductivity measurements of $Ba_2(In_{1-x}Ti_x)_2O_{5+x}\square_{1-x}$ ($x = 0.2$, 0.3 and 0.4) phases, in dry and wet N_2, shows that the best level of proton conductivity is obtained for BIT02 that is 1.1×10^{-3} S cm^{-1} at 450 °C for a very low level of hydration namely nOH ~ 0.075. The best conductivity level is not observed for fully hydrated phases reflecting a compromise between proton diffusion which increases with temperature and the protons concentration which decreases with temperature.

References

[1] H. Iwahara, H. Uchida, K. Morimoto, J. Electrochem. Soc. 137 (1990) 462–465.
[2] K. Xie, Q.L. Lin, Y.Z. Jiang, J.F. Gao, X.Q. Liu, G.Y. Meng, J. Power Sources 170 (2007) 38–41.
[3] N. Bonanos, B. Ellis, M.N. Mahmood, Solid State Ionics 44 (1991) 305–311.
[4] N. Taniguchi, K. Hatoh, J. Niikura, T. Gamo, Solid State Ionics 53–56 (1992) 998–1003.
[5] N. Maffei, L. Pelletier, A. Mctarlan, J. Power Sources 136 (2004) 24–29.
[6] N. Ito, M. Iijima, K. Kimura, S. Iguchi, J. Power Sources 152 (2005) 200–203.
[7] Q.L. Ma, R.R. Peng, Y.J. Lin, J.F. Gao, G.Y. Meng, J. Power Sources 161 (2006) 95–98.
[8] T. Hibino, A. Hashimoto, M. Suzuki, M. Sano, J. Electrochem. Soc. 149 (2002) A1503–A1508.
[9] L. Pelletier, A. McFarlan, N. Maffei, J. Power Sources 145 (2005) 262–265.
[10] A. Tomita, T. Hibino, M. Sano, Electrochem. Solid State Lett. 8 (2005) A333–A336.
[11] A. Tomita, K. Tsunekawa, T. Hibino, S. Teranishi, Y. Tachi, M. Sano, Solid State Ionics 177 (2006) 2951–2956.
[12] Y. Akimune, K. Matsuo, H. Higashiyama, K. Honda, M. Yamanaka, M. Uchiyama, M. Hatano, Solid State Ionics 178 (2007) 575–579.
[13] S.Y. Wang, J.L. Luo, A.R. Sanger, K.T. Chuang, J. Phys. Chem. C 111 (2007) 5069–5074.
[14] Y. Lin, R. Ran, Y. Zheng, Z. Shao, W. Jin, N. Xu, J. Ahn, J. Power Sources 180 (2008) 15–22.
[15] H. Iwahara, T. Yajima, T. Hibino, H. Ushida, J. Electrochem. Soc. 140 (1993) 1687–1691.
[16] R.R. Peng, Y. Wu, L.Z. Yang, Z.Q. Mao, Solid State Ionics 177 (2006) 389–393.
[17] V. Jayaraman, A. Magrez, M. Caldes, O. Joubert, M. Ganne, Y. Piffard, L. Brohan, Solid State Ionics 170 (2004) 17.
[18] V. Jayaraman, A. Magrez, M. Caldes, O. Joubert, F. Taulelle, J. Rodriguez-Carvajal, Y. Piffard, L. Brohan, Solid State Ionics 170 (2004) 25.
[19] J. Rodríguez-Carvajal, Physica B 192 (1993) 55, see also http://www-llb.cea.fr/fullweb/fp2k/fp2k.htm.
[20] T. Roisnel, J. Rodríguez-Carvajal, in: R. Delhez, E.J. Mittenmeijer (Eds.), Materials Science Forum, Proc. of the 7th European Powder Diffraction Conference (EPDIC 7), 2000, p. 118, see also http://www-llb.cea.fr/fullweb/winplotr/winplotr.htm.
[21] T. Norby, Y. Larring, Curr. Opin. Solid State Mater. Sci. 2 (1997) 593.
[22] K.D. Kreuer, Solid State Ionics 125 (1999) 285.
[23] S. Noirault, S. Celerier, O. Joubert, M.-T. Caldes, Y. Piffard, Solid State Ionics 178 (2007) 1353.
[24] G.B. Zhang, D.M. Smyth, Solid State Ionics 82 (1995) 153.
[25] H. Inaba, H. Tagawa, Solid State Ionics 83 (1996) 1.
[26] K.D. Kreuer, T. Dippel, Y.M. Baikov, J. Maier, Solid State Ionics 86 (1996) 613.